GEM TN-92-202

New Approach to Muon System Alignment

G. Mitselmakher & A. Ostapchuk
SSC Laboratory

October 2, 1992

Abstract:

New approach to the GEM muon system alignment is proposed. Projective straightness monitors readings completed with suitable interpolation procedures are used for correction of high momentum muon sagitta.

NEW APPROACH TO MUON SYSTEM ALIGNMENT

G.Mitselmakher A.Ostapchuk

October 2, 1992

Abstract

New approach to the GEM muon system alignment is proposed. Projective straightness monitors readings completed with suitable interpolation procedures are used for correction of high momentum muon sagitta.

1. Introduction
   - muon momentum resolution requirements
   - sagitta measurement accuracy
   - alignment tolerances

2. Concept of new approach
   - L3 alignment
   - present GEM alignment scheme
   - straightness monitors readings as information for sagitta correction
   - goals of new approach
     - softening of alignment requirements
     - current control of muon system changings, vibrations
     - correction of muon chamber deformations

3. Procedure for sagitta correction; minimal scheme
   - straightness monitor measures false sagitta
   - role of projectivity
   - interpolation within rectangle
   - geometrical setup: minimal scheme
   - formula for 4-point option

4. Monte Carlo calculations
   - Monte Carlo program assumptions

- corrected false sagitta: different shifts and rotations of rigid muon chambers
- insufficiency of minimal scheme

5. 6-point option
   - formula for 6-point option
   - Monte Carlo calculations

6. Chamber deformations
   - thermal deformations
   - torque
   - gravitational sag

7. Accuracy caused by non-projectivity
   - non-projectivity of particles trajectories
   - non-projectivity of monitor lines-of-sight

8. Non-bending monitor measurements
   - monitor readings self-consistency tests
   - control of any chamber movement by only four monitors

9. Alignment requirements
   - placement and measurement requirements
   - local alignment
     - momentum measurment
     - trigger
     - dynamic range of monitors
   - global alignment
     - momentum direction
     - mass measurement
     - dynamic range of monitors

10. Conclusions
    - drastically softened requirements
    - correction of muon chamber deformations
    - self-consistency tests

11. Acknowledgments

1. Introduction

For high momentum muons we can use the following parametrization of muon transverse momentum resolution:

$$\Delta p_t/p_t = \sigma_p p_t.$$

The transverse momentum of the muon is reconstructed by measuring the sagitta:

$$S[mm] = 37.5\frac{B[T]L^2[m]}{p_t[GeV]} = \frac{750mm}{p_t[GeV]} \text{ for barrel.}$$

GEM muon resolution goals are [1]

$\sigma_p \leq 10^{-4}$ for barrel,

$\sigma_p \leq 2.10^{-4}$ for endcaps.

So: $\delta S = 750mm * \sigma_p$ or

δS= 75μm for barrel,

δS for endcaps $\simeq \delta S$ for barrel.

The total sagitta resolution depends on bending coordinates resolution in all three superlayers:

$$\delta S = \sqrt{\frac{\sigma_1^2+\sigma_3^2}{4} + \sigma_2^2}$$

The measurement error in the bending (x) direction of each superlayer is given by:

$$\sigma_i = \sqrt{\frac{\sigma_{int}^2}{n_i * e_i} + \sigma_{algn}^2 + \sigma_{mcs}^2},$$

where σ_{int} is the intrinsic detector resolution(100μm for barrel,75μm for endcaps), n_i- the number of layer in each superlayer (8/8/4 -barrel, 4/4/4 -endcap), e_i- the efficiency of layer, σ_{algn} - alignment error, and σ_{mcs} - the error due to multiscattering (essential for middle superlayer and moderate momentum).

In [2] the limitation of σ_{algn} was studied. The requirement δS= 75μm implies the requirement $\sigma_{algn} \leq 25\mu m$. The same tolerance for this value was suggested in [3].

From this evaluation it is concluded that placement accuracies on the order of a few tens of microns is required if an alternate strategy is not developed.

2. Concept of new approach

Other HEP experiments have addressed alignment requirements comparable to GEM. L3, faced with a similar task, solved it successfully although at a smaller scale. The alignment method used by L3 physically placed muon chambers to required tolerances and measured these positions with similar accuracies.

The present GEM alignment configuration [2,3,4] is based on the L3 experience. However, since GEM is much larger than L3, a modified strategy is needed. The basic concept is to **not** accurately place the Tests for straightness monitors measurements are suggested. muon chambers with few-tens micron accuracy, but rather to rely upon very accurate ($\sim 25\mu$m) measurement of muon chamber positions.

We propose the following approach.

There is no necessity to measure mutual displacements of muon superlayers with this high accuracy. Straightness monitor readings contain immediate information about high momentum muon false sagitta. This information can be used to calculate precise muon sagitta. We propose a procedure for this calculation.

The main goal of this approach is to soften the placement requirements. It results in decreasing the GEM muon system cost and increasing its reliability.

The next goal is to correct high momentum muon sagitta during GEM operation time using changing straightness monitor readings caused by vibrations of the muon system.

Finally, we hope this approach will allow, to some extent, the correction of muon momentum measurement errors, caused by muon chamber deformations such as torque, gravitational sag, and linear thermal distortion.

3. Procedure for sagitta correction; minimal scheme

The proposed realization of our foregoing goals is based on three principles.

False sagitta measurement. Sagitta is a parameter which characterizes trajectory deviation from a straight line. By definition any straightness monitor measures a parameter characterizing deviation of muon chambers from a straight line. Therefore for particles whose trajectories are near monitor location there is a direct measurement of their false sagitta.

Projectivity. Trajectories of high momentum muons have a radial projective direction: their impact parameter to the interaction point (IP) is very small ($\sim 1cm$). If straightness monitor arrays are arranged in this projective direction they would measure exactly false sagittas of high momentum muons.

Interpolation. Any projective particle intersecting outer superlayer within some rectangular module is fully determined by two coordinates of the intersection point (see Fig.1). So, within the solid angle limited by the given module, we have a function FS(x,z) - false sagitta dependence on intersection point coordinates. We propose to arrange projectively chambers of different superlayers so they will form towers of the GEM muon system (one of them shown in Fig. 2.) Inside one tower the function FS(x,z) will be a smooth function of coordinates x and z. Monitors placed on the edges of the rectangle provide us with measured values of this function at their sites (see Fig.2 where one possible straightness

monitor scheme is displayed). Therefore we can use an interpolation of measured values inside the tower.

It's necessary to stress here again that we don't calculate the magnitude of real displacements and rotations. This task requires much more information. We interpolate only the minimum amount of information that is important to us: false sagitta. This minimizes the number of monitors.

The minimal scheme includes four straightness monitors at the rectangle corners. They provide us with four values of the function FS. Our task is to interpolate these values to the internal points.

There is an elegant geometrical representation of most suitable for our purposes interpolation (see Fig.3):

$$FS\,|_P = \frac{FS_1 * S_1 + FS_2 * S_2 + FS_3 * S_3 + FS_4 * S_4}{S_{tot}}$$

Here:
FS_i is the measured value of false sagitta at the i-th vertex;
S_i is the area of the rectangle opposite to the i-th vertex;
S_{tot} is the area of the total rectangle.

4. Monte Carlo calculations

To verify this procedure of sagitta correction, the Monte Carlo program was written. Calculations were made using the following assumptions:

- the muon tower has the following dimensions:
  z-length of the outer superlayer module is 4m,
  ϕ-angle of the tower is $360^0/16$;
- trajectory of particles are the straight lines, so measured sagitta is equal to false sagitta;
- straightness monitors have 25μm resolution;
- muon chambers have perfect resolution;
- each superlayer is shifted and rotated independently;
- particles are distributed uniformly inside the solid angle;
- values of chamber shifts and rotations are distributed uniformly within tolerances.

The calculated dependences of sagitta corrected values on the values of false sagitta for different chamber movements are represented in Figs. 5 through 8:

Fig. 5 demonstrates that "plane" shifts of muon chambers along x- and z-directions (see Fig.1) are corrected completely. The dispersion of corrected sagitta approximately 10μm is determined fully by the value of straightness monitors resolution;

Rotations of muon chambers around y-axis with tolerance $\leq \pm 3mrad$ are also corrected entirely (see Fig.6);

Combination of the two previous movements which do not change muon chamber planes is controlled by this method as well (see Fig.7);

"Radial movements": shifts of muon chambers along y-axis and rotations around x-axis can also be corrected. Fig.8 demonstrates the same tolerances as for plane movements;

This interpolation describes false sagittas generated by shifts and rotations in the module plane and in radial direction.

But what about z-axis rotations? Calculations show that, in this case, the procedure is absolutely inadequate (see Fig.9)

The reason is clear. With the four monitors at each corner of the rectangle this rotation appears to the straightness monitors as a shift in the x-direction. This is shown in Fig.4.

5. 6-point option

To solve this problem, two more monitors are introduced at the middle of the x-sides.

Now there are six measured values of the false sagitta. In this case, suitable interpolation quadratic interpolation on opposite x-edges and then linear interpolation along the z-axis.

Namely, place the 5-th monitor between the 1-st and the 3-rd monitors and the 6-th monitor - between the 2-nd and the 4-th (see Fig.3).

First, using standard Lagrange 3 point interpolation, we calculate $FS\mid_{P_1}$ using values FS_1, FS_5 and FS_4:

$$FS\mid_{P_1} = FS_1 * \frac{(X_{P_1}-X_5)*(X_{P_1}-X_4)}{(X_1-X_5)*(X_1-X_4)} + FS_5 * \frac{(X_{P_1}-X_1)*(X_{P_1}-X_4)}{(X_5-X_1)*(X_5-X_4)} + FS_4 * \frac{(X_{P_1}-X_1)*(X_{P_1}-X_5)}{(X_4-X_1)*(X_4-X_5)}$$

Then, we repeat the procedure for values FS_2, FS_6 and FS_3 and the point P_2:

$$FS\mid_{P_2} = FS_2 * \frac{(X_{P_2}-X_6)*(X_{P_2}-X_3)}{(X_2-X_6)*(X_2-X_3)} + FS_6 * \frac{(X_{P_2}-X_2)*(X_{P_2}-X_3)}{(X_6-X_2)*(X_6-X_3)} + FS_3 * \frac{(X_{P_2}-X_2)*(X_{P_2}-X_6)}{(X_3-X_2)*(X_3-X_6)}$$

Finally, we linearly interpolate values $FS\mid_{P_1}$ and $FS\mid_{P_2}$ to the point P:

$$FS\mid_{P} = FS\mid_{P_1} * \frac{(Z_P-Z_{P_2})}{(Z_{P_1}-Z_{P_2})} + FS\mid_{P_2} * \frac{(Z_P-Z_{P_1})}{(Z_{P_2}-Z_{P_1})}$$

Fig.10 demonstrates that this interpolation procedure controls rotations about the z-axis.

6. Chamber deformations

Straightness monitor measures false sagitta which is caused by relative displacements between superlayers. These displacements can be the result of both alignment errors and chamber deformations. The methodology we propose corrects for these motions to the extent defined below.

Correction of false sagitta due to thermal expansion/contraction is represented in Fig. 11. Relative temperatures of different superlayers are varied over large intervals, $\pm 100^0 C$. The assumed coefficient of linear thermal expansion is $10\mu m/m * grad$.

Torsion deformations of muon chambers (see Fig.12c) are also controlled by this method. Figs.12a,b demonstrate that an applied torque of $\Psi_{torque} \leq \pm 10 mrad$ can be accurately corrected.

Gravitational sag is not accurately corrected by the 6-point technique. The sagitta

error has a maximum value of order $\Delta h * \Phi_{sect}/2$, where Δh is the magnitude of the gravitational sag and Φ_{sect} is the tangent of the sector angle (see Fig.2). The error can be improved by one of the following options.

First, we can add two more monitors on the long (z-) sides of the muon chambers, bringing the total number of monitors to 8 per tower (see Fig.13a).

Second, we can measure the magnitude of the gravitational sag for all chambers in a tower by straightness monitors located on their surfaces (see Fig.13b).

In both cases we believe we will control this kind of deformation.

Now we can apply rigid body movements and thermal and torque deformationsand calculate corresponding sagitta errors. Fig.14 shows results which have been corrected by the 6-point interpolation. Displacement assumptions were: Dx,Dy,Dz$\leq \pm 5mm$; $Sx, Sy, Sz \leq \pm 3mrad$,$\Delta t^0 \leq \pm 5^0$, $\Psi_{torque} \leq \pm 3mrad$. Resolution of the corrected sagitta is better than 25μm.

7. Accuracy caused by non-projectivity

It is necessary to check the accuracy of the proposed procedure to inevitable non-projectivity. There are two kinds of potential non-projectivity in our case.

a. The non-projectivity of particle trajectories due to multiple scattering, curvature in the magnetic field, and finite longitudinal size of bunch. Fig.15 shows the accuracy of this method which assumes the tolerances of Fig.14 and displacements relative to IP of $\Delta X_{IP} \leq \pm 1cm; \Delta Z_{IP} \leq \pm 5cm$.

b. There are two types of non-projectivity of straightness monitors.

First, the muon tower has a sharp vertex, but this point does not coincide with the interaction point (IP). Our procedure is accurate with respect to this type of non-projectivity up to 3 cm of misalignment between the IP and the tower vertex (see Fig.16).

Second, straightness monitors arrays can be "defocused". The interpolation procedure permits relative angular errors of these monitors up to 3 mrad without introducing significant error (Fig.17).

8. Non-bending monitor measurements

Thus far we have used only bending direction measurements of straightness monitors. However LED/lens straightness monitor system can also measure non-bending deviation with the same sensor. Thus we have additional measurements of another function (say, non-straightness) NS(x,z).

These measurements are very significant and can be used for various purposes.

First, they make the system of monitor readings redundant. Therefore they provide us with some correlations between monitor readings, which have to be fulfilled if the monitor system is in order.

Namely, we can represent interpolation functions as polynomials:

$$FS^{(4)}(x,z) = a_{00}^{(4)} + a_{10}^{(4)}x + a_{01}^{(4)}z + a_{11}^{(4)}xz$$

$$FS^{(6)}(x,z) = a_{00}^{(6)} + a_{10}^{(6)}x + a_{01}^{(6)}z + a_{11}^{(6)}xz + a_{20}^{(6)}x^2 + a_{21}^{(6)}x^2z$$

Different terms are different linear combinations of FS_i (measured values of false sagitta) and therefore they depend on different movements. So,

a_{00} is determined by shift along the x-axis;

a_{01} is determined by rotation around the y-axis;

a_{10} is determined by rotation around the x-axis;

a_{20} is determined by rotation around the z-axis;

We can apply the same interpolation procedure to the function NS(x,z) and get similar polynomials:

$$NS^{(4)}(x,z) = b_{00}^{(4)} + b_{10}^{(4)}x + b_{01}^{(4)}z + b_{11}^{(4)}xz$$

$$NS^{(6)}(x,z) = b_{00}^{(6)} + b_{10}^{(6)}x + b_{01}^{(6)}z + b_{11}^{(6)}xz + b_{20}^{(6)}x^2 + b_{21}^{(6)}x^2z$$

The coefficients of these polynomials depend on shifts and rotations of muon modules in different ways, but the shifts and rotations are the same in both cases! So, there must be correlations between coefficients a_{ij} and b_{ij}:

b_{10} is fully correlated with a_{01} (see Fig.18),

b_{01} is slightly correlated with a_{11} (see Fig.19);

and most interesting, if there are no torque deformations of muon modules,

b_{11} is fully correlated with a_{20} (Fig.20, but see Fig. 21).

The last correlation means we are able to correct rotation around z-axis using only four straightness monitors. This is the second application of monitor measurements of non-bending deflections.

9. Alignment requirements

We would like to stress the sharp distinction between placement and measurement accuracy requirements. The only requirement for monitor measurement accuracy is that it must be better than 25μm.

There are two types of placement or proper position requirements: 1) relative po-

sitioning of the muon chambers within one muon tower, or *local requirements*, and 2) requirements for positioning of different muon towers with respect to IP and to the central tracker, or *global requirements*.

Local requirements are determined, in principle, by three factors: measurements of high-energetic muon momenta, trigger roads and dynamic range of monitors. We did not examine the last two issues in our proposal, they were studied in [2,3]. Comparison with these estimations shows that our approach softens placement requirements dictated by momentum measurements so much, that placement requirements are completely determined by trigger roads and dynamic range of monitors.

The only global requirement produced by our approach is the rather soft tolerance on the projectivity of a muon tower: focus can be shifted from the IP to not more than 30mm in each direction (see Fig.16).

Other global requirements depend on such factors as muon momentum direction measurement and di-muon mass measurement. These requirements were analysed in [2,3].

10. Conclusions

The main conclusions are the following:

- Alignment tolerances are drastically increased up to 5mm in bending direction.
- Most probable muon chamber deformations are shown to be correctable.
- Self-consistency tests for straightness monitor readings are proposed.

11. Acknowledgments

We gratefully acknowledge Mike Marx and Rick Sawicki for their helpful comments on the content of this note, and Linda Fowler, for her assistance during preparation for publication.

References

1. GEM Letter of Intent, SSCL-SR-1184

2. Mitselmakher G. and Zhukov V.,"Alignment Requirements to Muon System", GEM internal note TN-92-120

3. Paradiso J.,"Alignment Requirements for the GEM Muon Detector", GEM internal note TN-92-125

4. GEM Baseline 1, GEM TN-92-76

Figures

Fig.1 Coordinate System

Fig.2 Muon Tower

Fig.3 Geometrical Representation of Interpolation Formula

Fig.4 Insufficiency of 4-Point Option

Fig.5 Shifts of Muon Chambers: $Dx \leq \pm 1cm; Dz \leq \pm 1cm$
Fig.5a Corrected Sagitta(cm) vs False Sagitta(cm)
Fig.5b Corrected Sagitta(cm)

Fig.6 Rotations of Muon Chambers: $Sy \leq \pm 3mrad$
Fig.6a Corrected Sagitta(cm) vs False Sagitta(cm)
Fig.6b Corrected Sagitta(cm)

Fig.7 Shifts and Rotations of Muon Chambers: $Dx \leq \pm 1cm; Dz \leq \pm 1cm; Sy \leq \pm 3mrad$
Fig.7a Corrected Sagitta(cm) vs False Sagitta(cm)
Fig.7b Corrected Sagitta(cm)

Fig.8 Shifts and Rotations of Muon Chambers: $Dy \leq \pm 1cm; Sx \leq \pm 3mrad$
Fig.8a Corrected Sagitta(cm) vs False Sagitta(cm)
Fig.8b Corrected Sagitta(cm)

Fig.9 Rotations of Muon Chambers: $Sz \leq \pm 3mrad$; 4-Point Option
Fig.9a Corrected Sagitta(cm) vs False Sagitta(cm)
Fig.9b Corrected Sagitta(cm)

Fig.10 Rotations of Muon Chambers: $Sz \leq \pm 3mrad$; 6-Point Option
Fig.10a Corrected Sagitta(cm) vs False Sagitta(cm)
Fig.10b Corrected Sagitta(cm)

Fig.11 Temperature Scale Transformations of Muon Chambers: $\Delta t^0 \leq \pm 100^0$
Fig.11a Corrected Sagitta(cm) vs False Sagitta(cm)
Fig.11b Corrected Sagitta(cm)

Fig.12 Torque Deformations of Muon Chambers: $\Psi_{torque} \leq \pm 10mrad$
Fig.12a Corrected Sagitta(cm) vs False Sagitta(cm)
Fig.12b Corrected Sagitta(cm)
Fig.12c Picture of Torque Deformations

Fig.13a Control of Gravitation Sag by 8 Projective Monitors
Fig.13b Control of Gravitation Sag by 6 Projective and 3 Plane Monitors

Fig.14 Shifts and Rotations of Muon Chambers: $Dx, Dy, Dz \leq \pm 5mm$; $Sx, Sy, Sz \leq \pm 3mrad$; Deformations of Muon Chambers: $\Psi_{torque} \leq \pm 3mrad$, $\Delta t^0 \leq \pm 5^0$
Fig.14a Corrected Sagitta(cm) vs False Sagitta(cm)
Fig.14b Corrected Sagitta(cm)

Fig.15 Non-Projectivity of Particle Trajectory: $\Delta X_{IP} \leq \pm 1cm; \Delta Z_{IP} \leq \pm 5cm$
Shifts, Rotations and Deformations of Muon Chambers as for Fig.14
Fig.15a Corrected Sagitta(cm) vs False Sagitta(cm)
Fig.15b Corrected Sagitta(cm)

Fig.16 Deflection of Muon Tower Focus from Interaction Point: $X_{focus} = 3cm; Y_{focus} = 3cm; Z_{focus} = 3cm$; Shifts, Rotations and Deformations of Muon Chambers as for Fig.14
Fig.16a Corrected Sagitta(cm) vs False Sagitta(cm)
Fig.16b Corrected Sagitta(cm)

Fig.17 Deflection of Monitor Direction from Interaction Point: $\Delta\theta \leq \pm 3mrad$
Shifts, Rotations and Deformations of Muon Chambers as for Fig.14
Fig.17a Corrected Sagitta(cm) vs False Sagitta(cm)
Fig.17b Corrected Sagitta(cm)

Fig.18 b_{10} vs a_{01}

Fig.19 b_{01} vs a_{11}

Fig.20 b_{11} vs a_{02}; No Torsion

Fig.21 b_{11} vs a_{02}; Torsion: $\Psi_{torque} \leq \pm 3mrad$

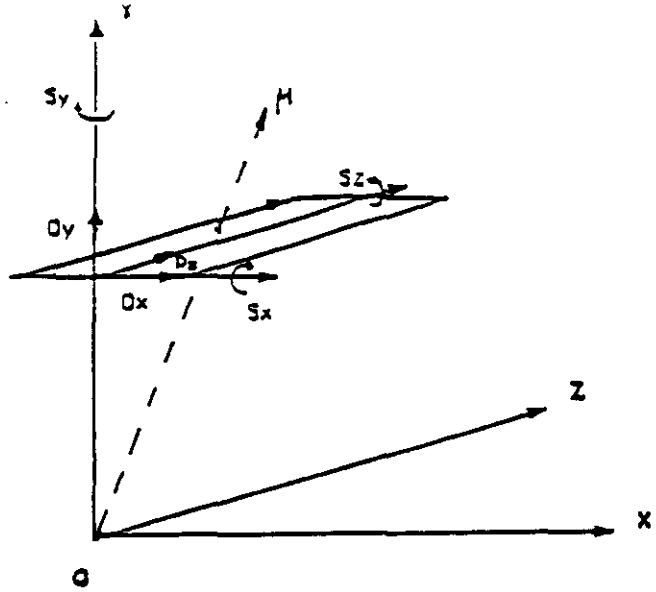

Fig.1 Coordinate System

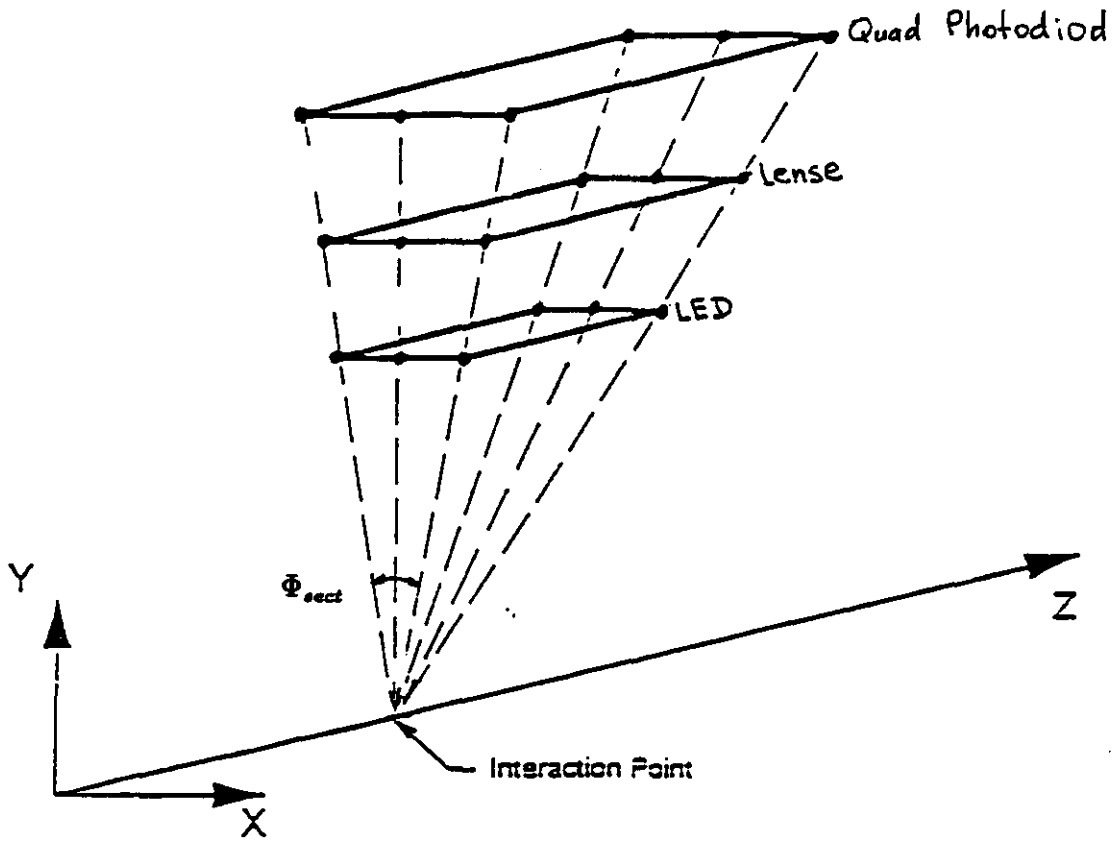

Fig.2 Muon Tower

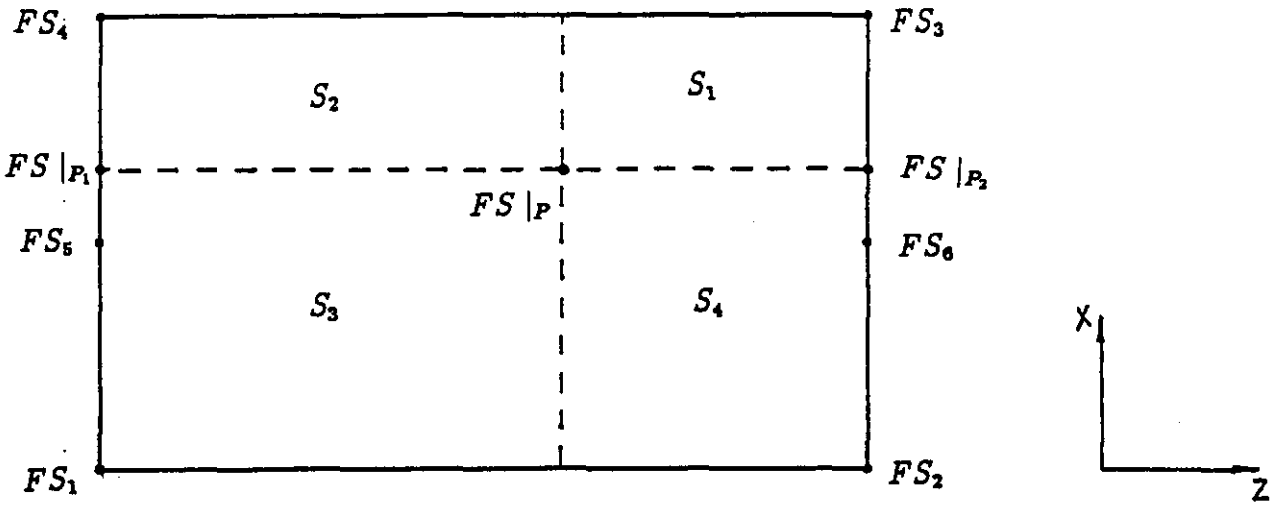

Fig.3 Geometrical Representation of Interpolation Formula

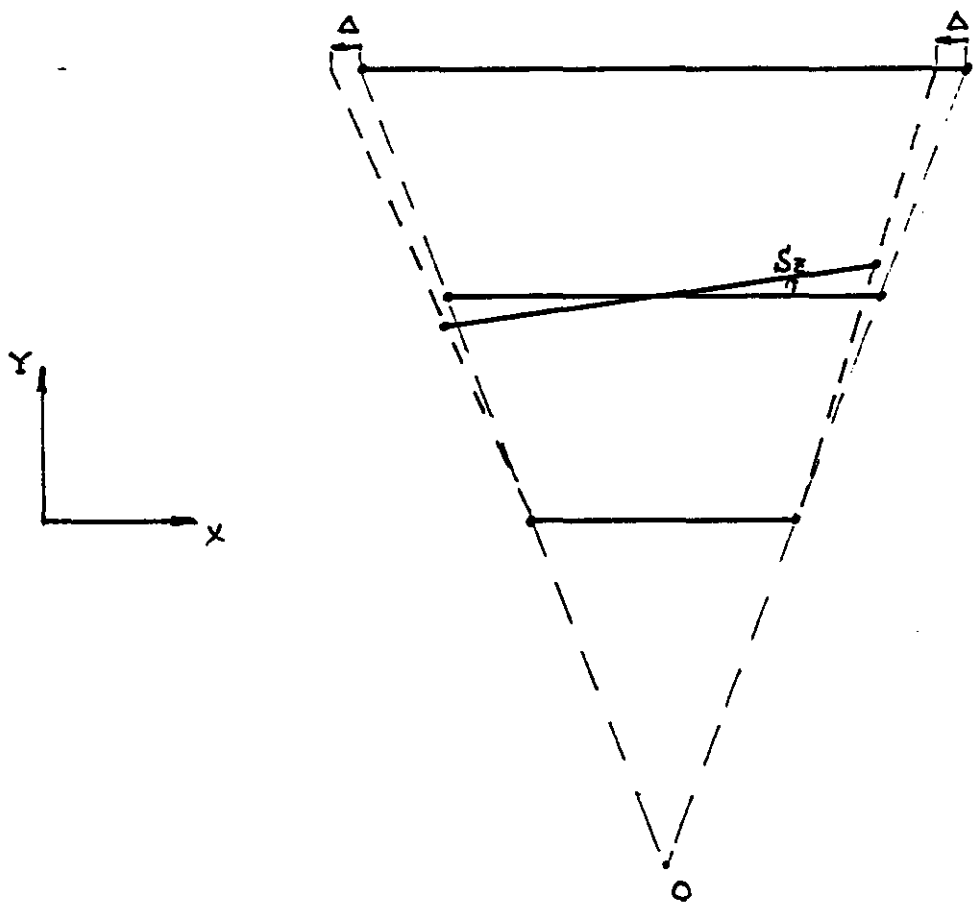

Fig.4 Insufficiency of 4-Point Option

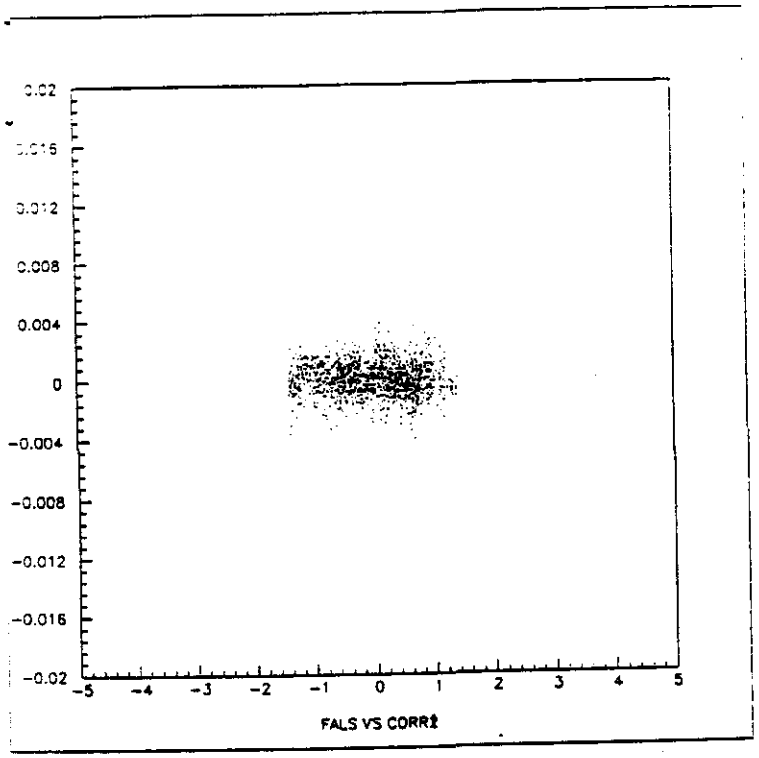

g.5a Corrected Sagitta(cm) vs False Sagitta(cm)

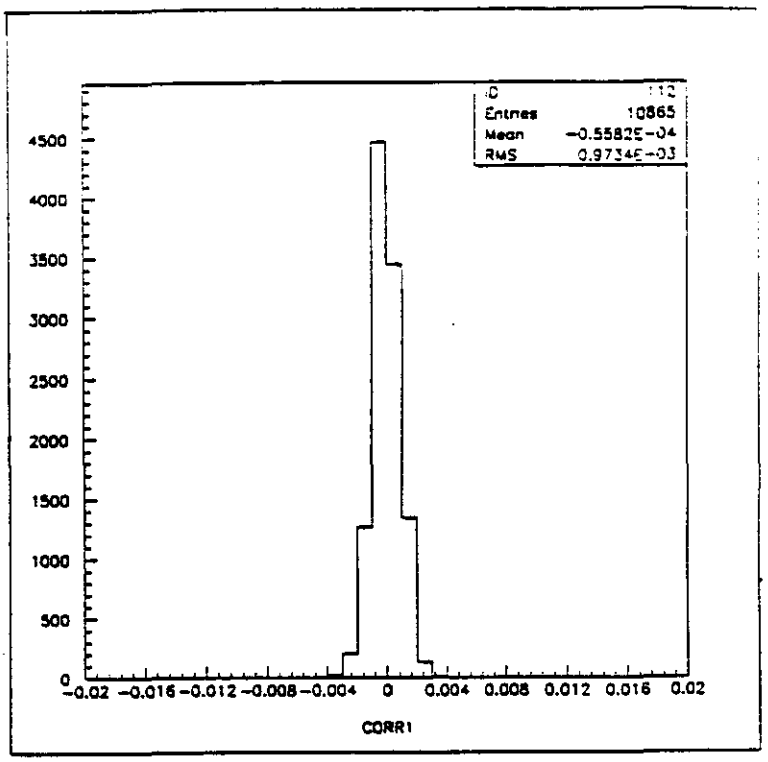

Fig.5b Corrected Sagitta(cm)

Shifts of Muon Chambers: $Dx \leq \pm 1cm; Dz \leq \pm 1cm$

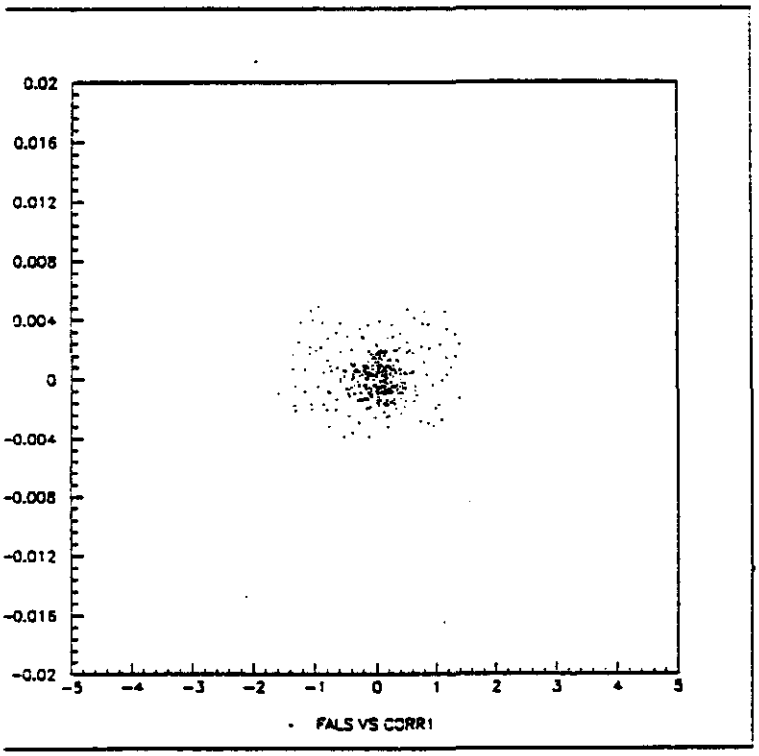

ig.6a Corrected Sagitta(cm) vs False Sagitta(cm)

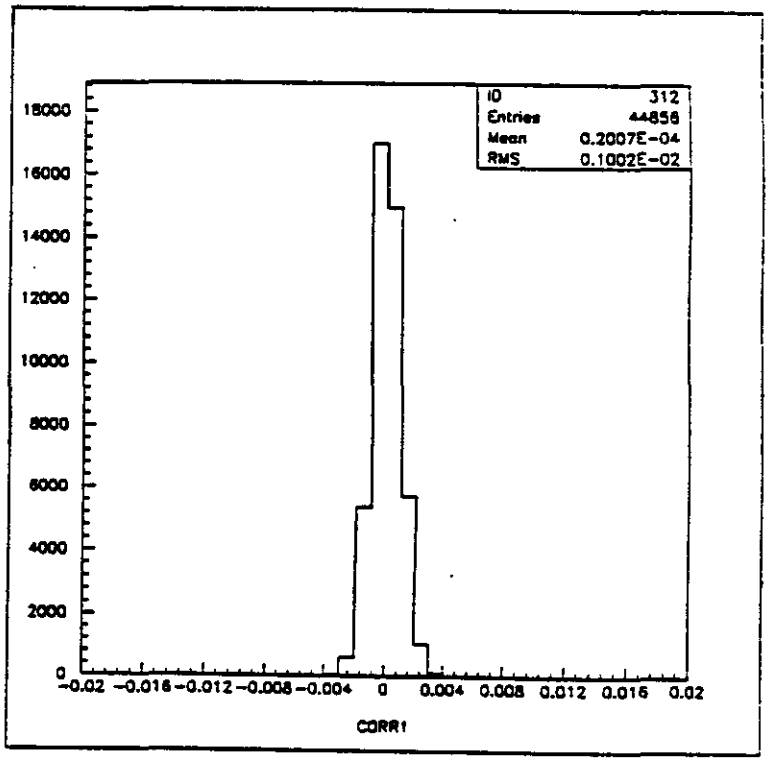

Fig.6b Corrected Sagitta(cm)

Rotations of Muon Chambers: $Sy \leq \pm 3mrad$

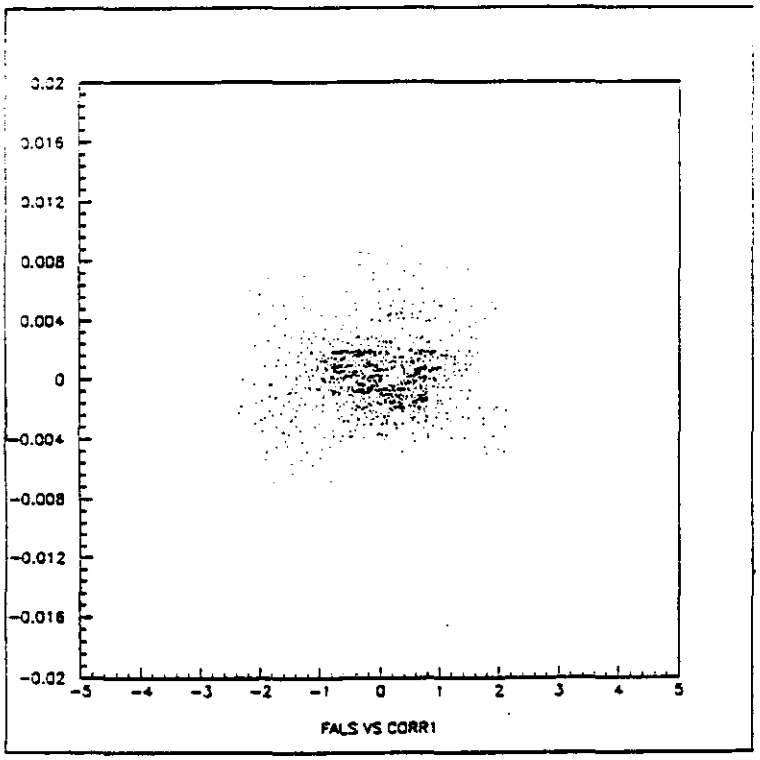

Fig.7a Corrected Sagitta(cm) vs False Sagitta(cm)

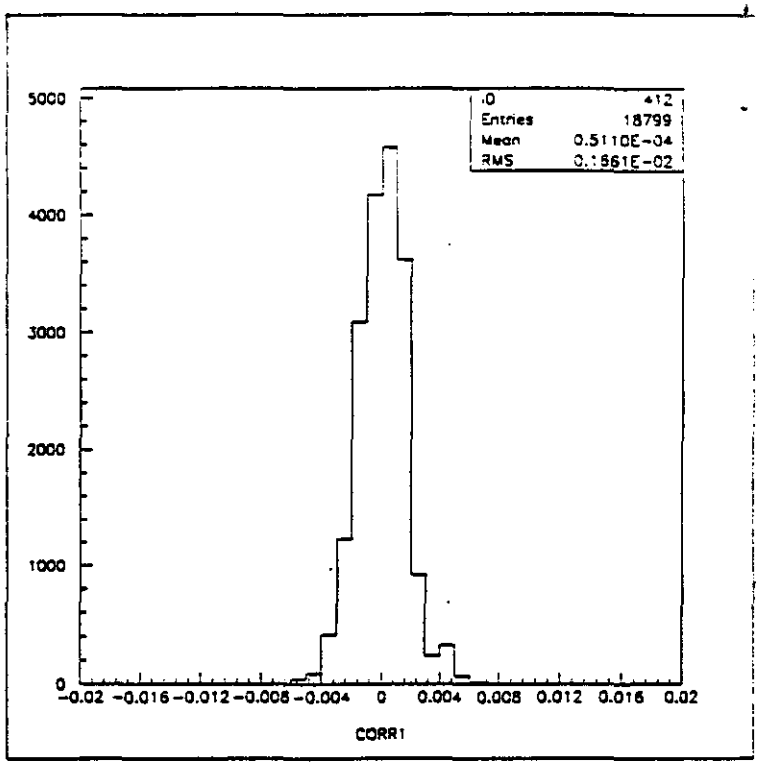

Fig.7b Corrected Sagitta(cm)

Shifts and Rotations of Muon Chambers: $Dx \leq \pm 1cm; Dz \leq \pm 1cm; Sy \leq \pm 3mrad$

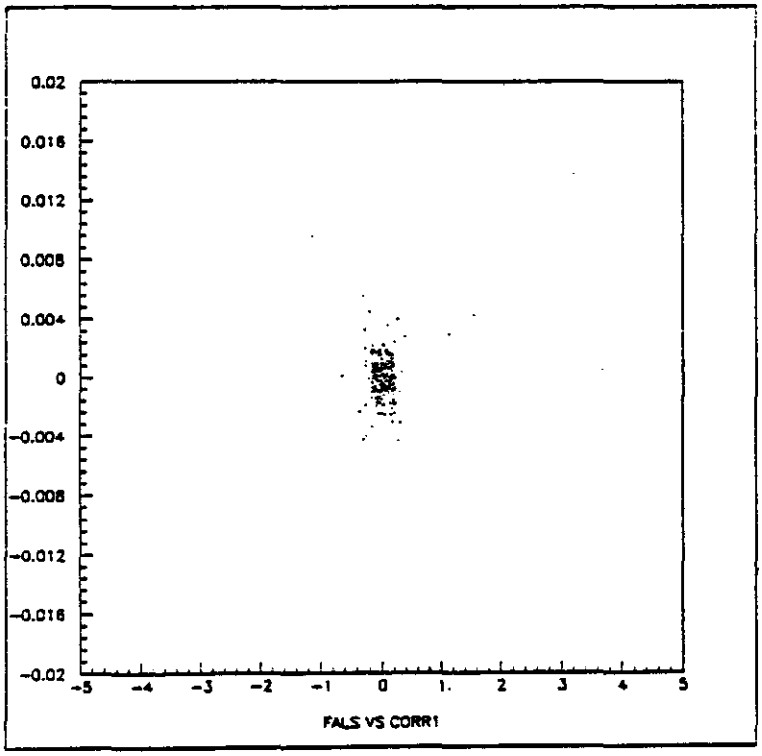

Fig.8a Corrected Sagitta(cm) vs False Sagitta(cm)

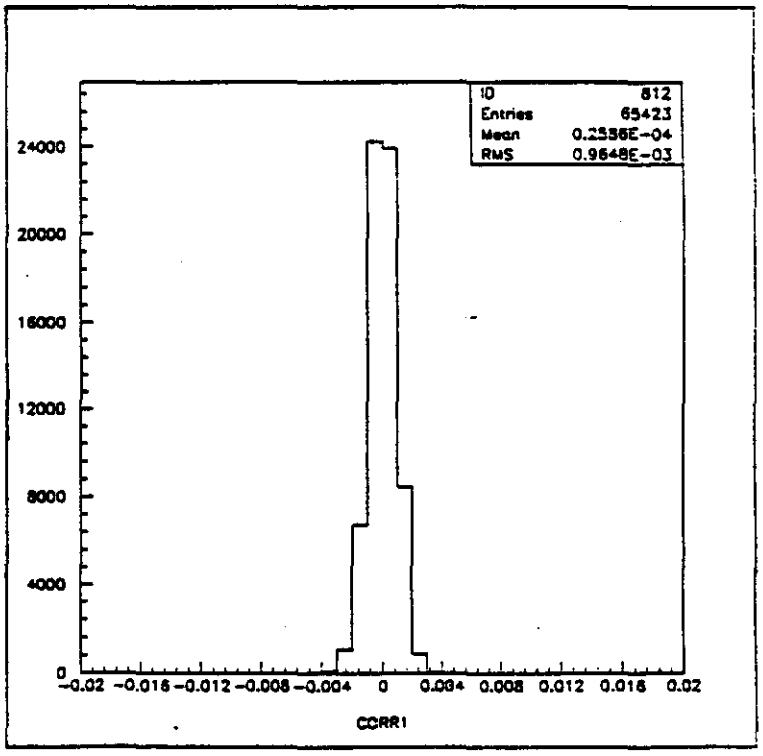

Fig.8b Corrected Sagitta(cm)

Shifts and Rotations of Muon Chambers: $Dy \leq \pm 1cm; Sx \leq \pm 3mrad$

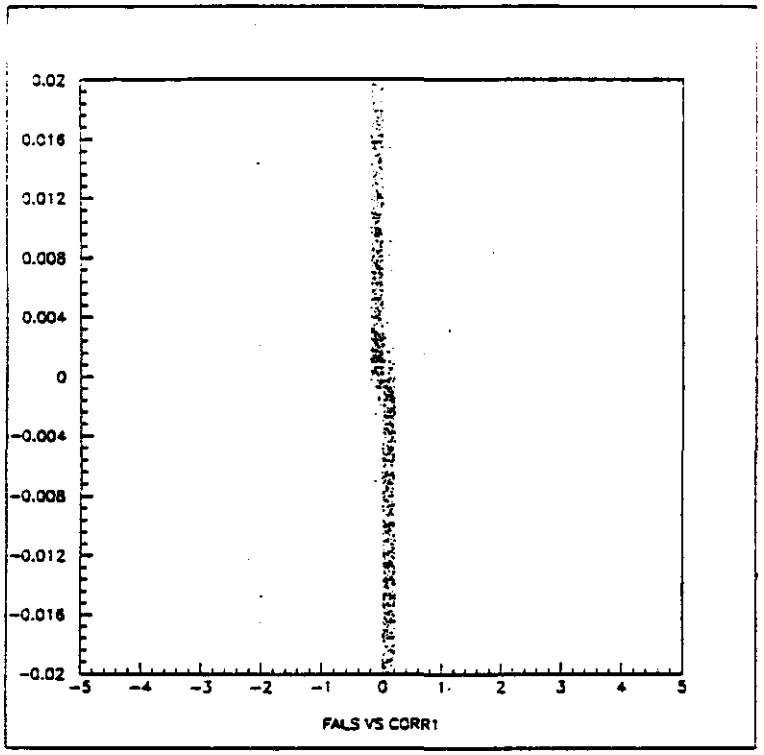

Fig.9a Corrected Sagitta(cm) vs False Sagitta(cm)

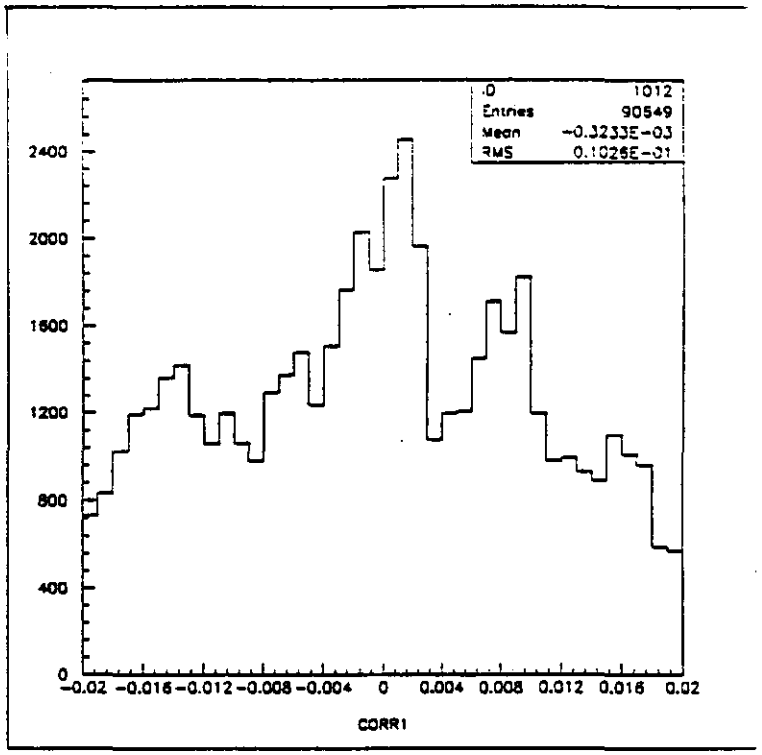

Fig.9b Corrected Sagitta(cm)

Rotations of Muon Chambers: $Sz \leq \pm 3mrad$; 4-Point Option

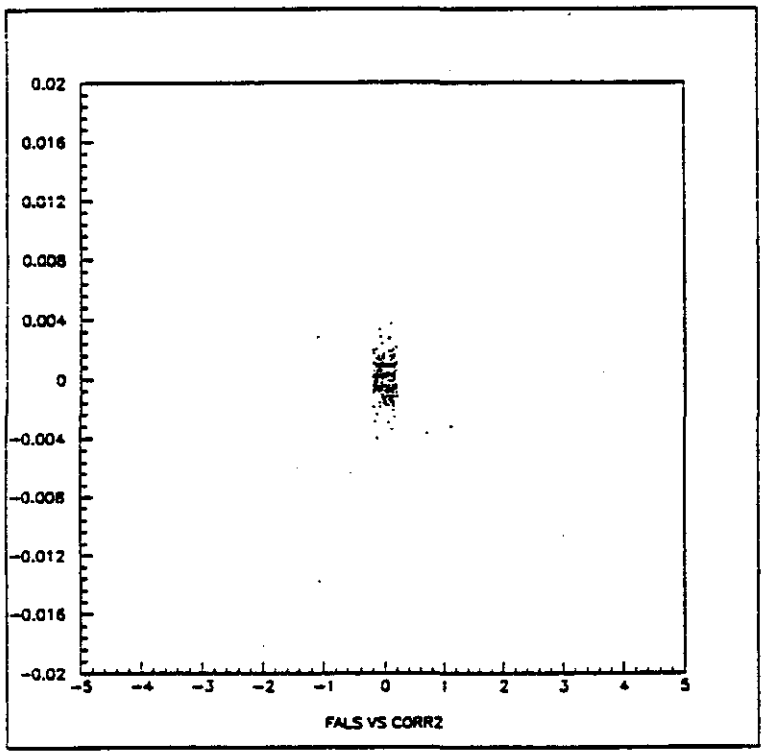

Fig.10a Corrected Sagitta(cm) vs False Sagitta(cm)

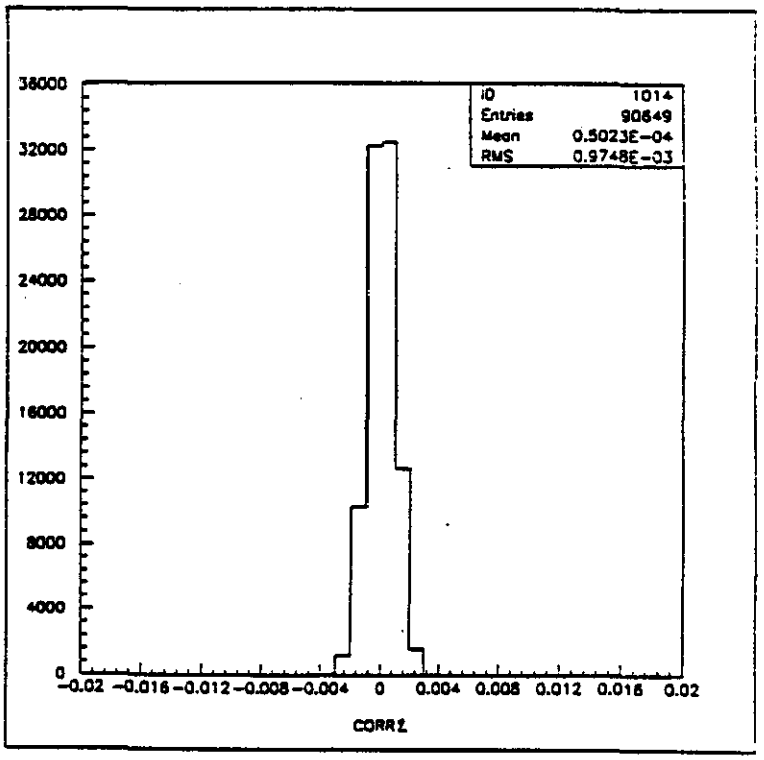

Fig.10b Corrected Sagitta(cm)

Rotations of Muon Chambers: $Sz \leq \pm 3mrad$; 6-Point Option

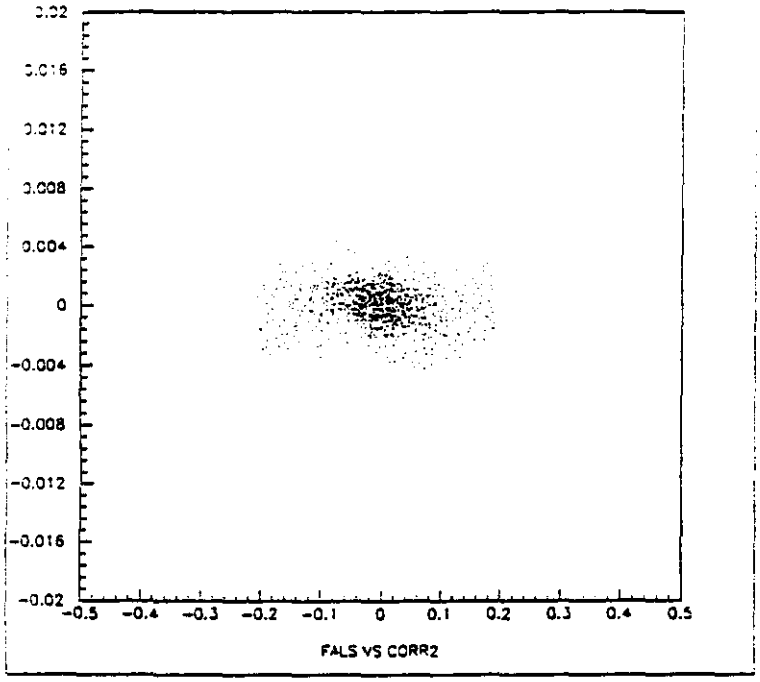

Fig.11a Corrected Sagitta(cm) vs False Sagitta(cm)

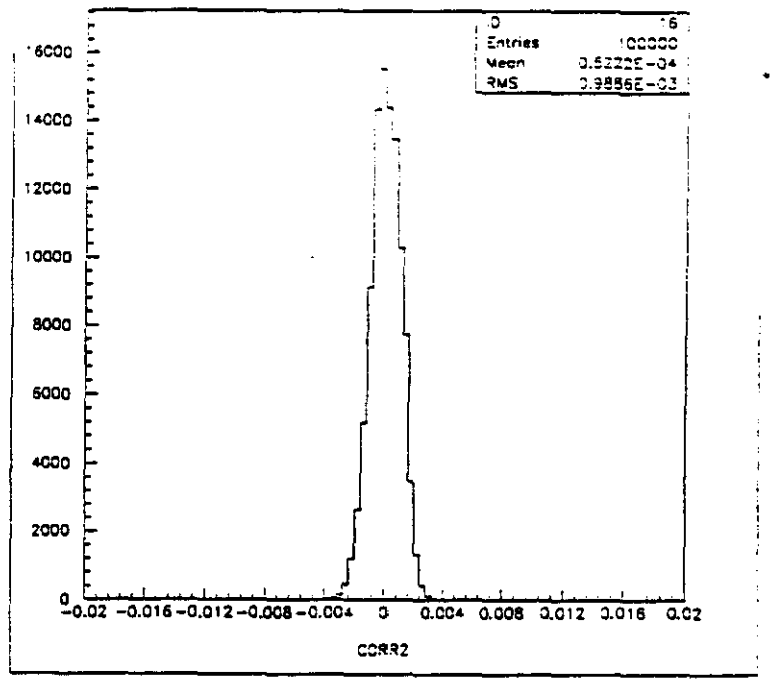

Fig.11b Corrected Sagitta(cm)

Temperature Scale Transformations of Muon Chambers: $\Delta t^0 \leq \pm 100^0$

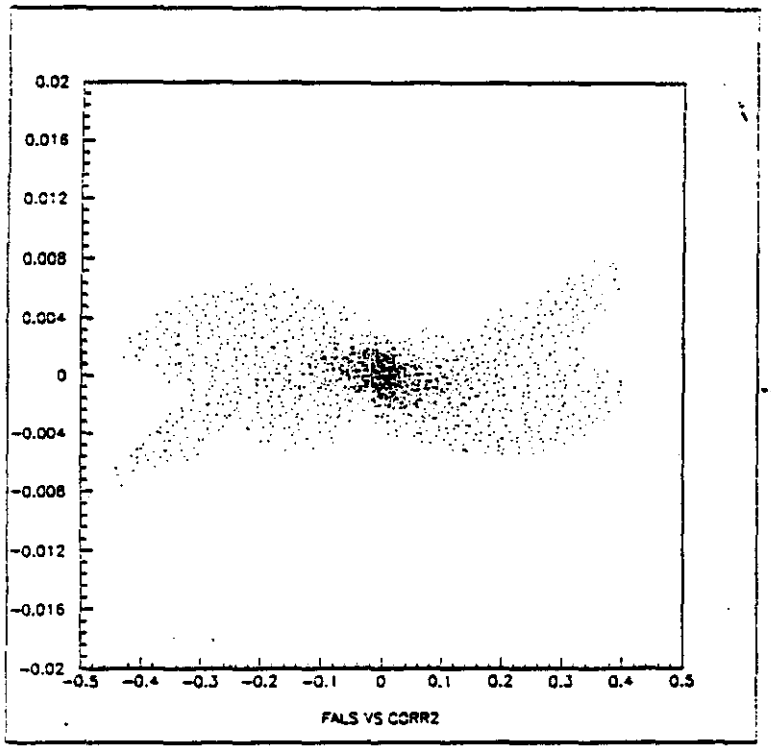

Fig.12a Corrected Sagitta(cm) vs False Sagitta(cm)

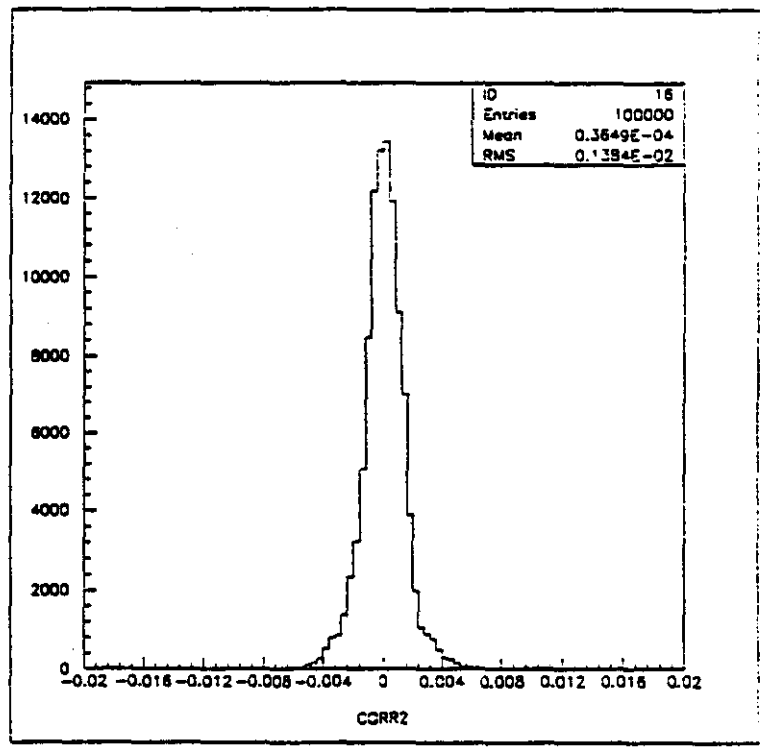

Fig.12b Corrected Sagitta(cm)

Torque Deformations of Muon Chambers: $\Psi_{torqe} \leq \pm 10 mrad$

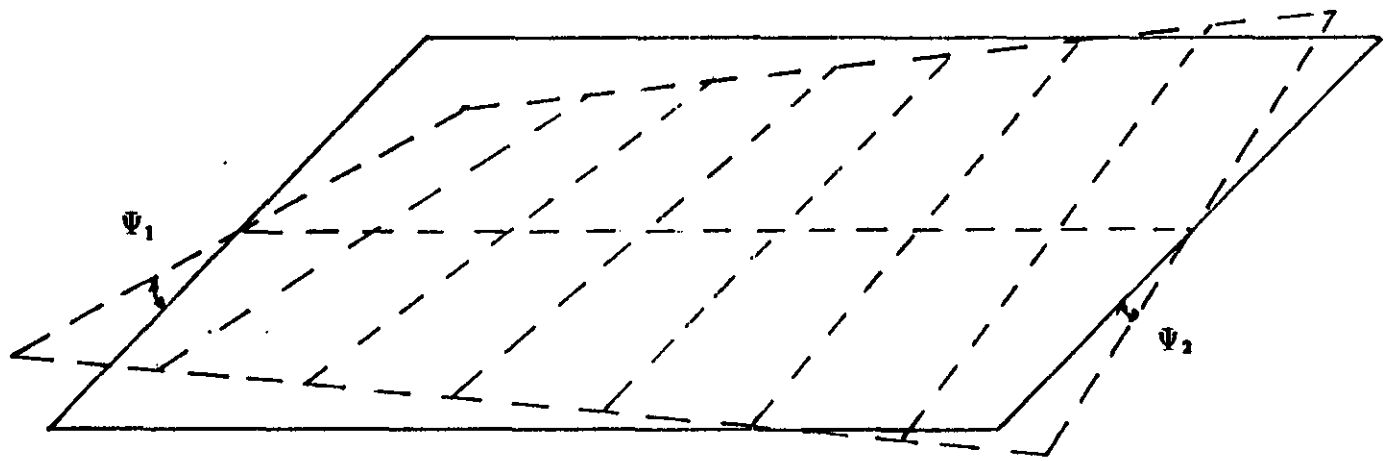

$$-\Psi_{torque} \leq \Psi_1 \leq \Psi_{torque}$$

$$-\Psi_{torque} \leq \Psi_2 \leq \Psi_{torque}$$

Ψ_1 and Ψ_2 change independently

Fig.12c Torque Deformations of Muon Chambers

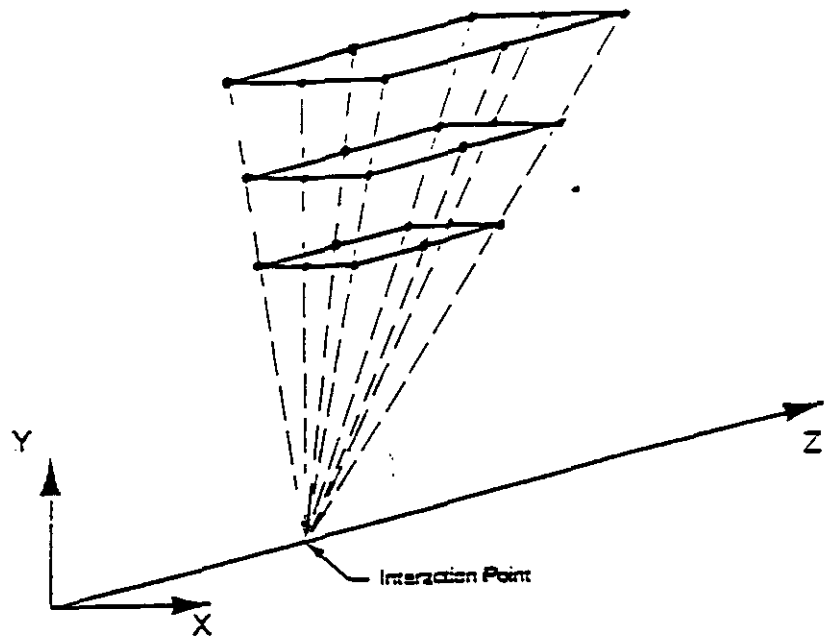

Fig.13a Control of Gravitation Sag by 8 Projective Monitors

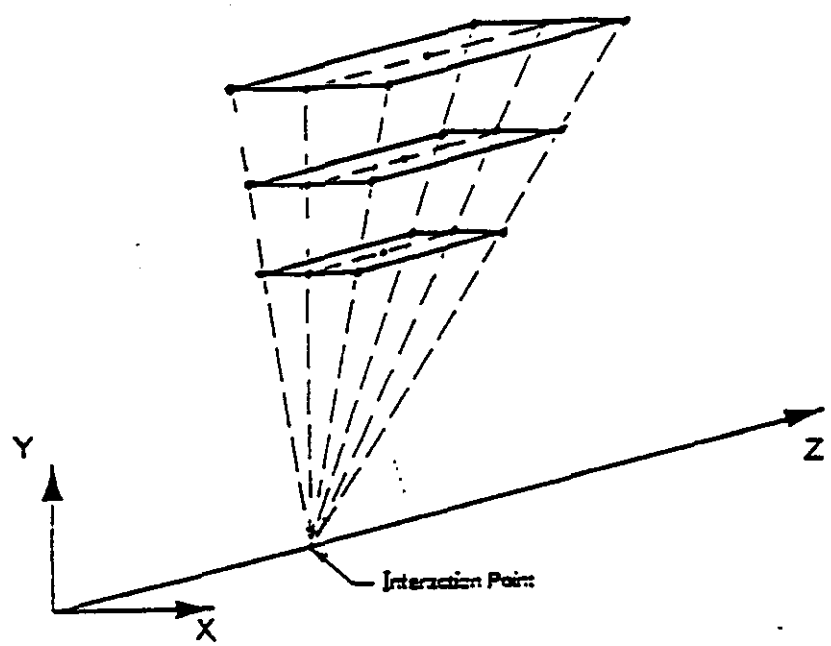

Fig.13b Control of Gravitation Sag by 6 Projective and 3 Plane Monitors

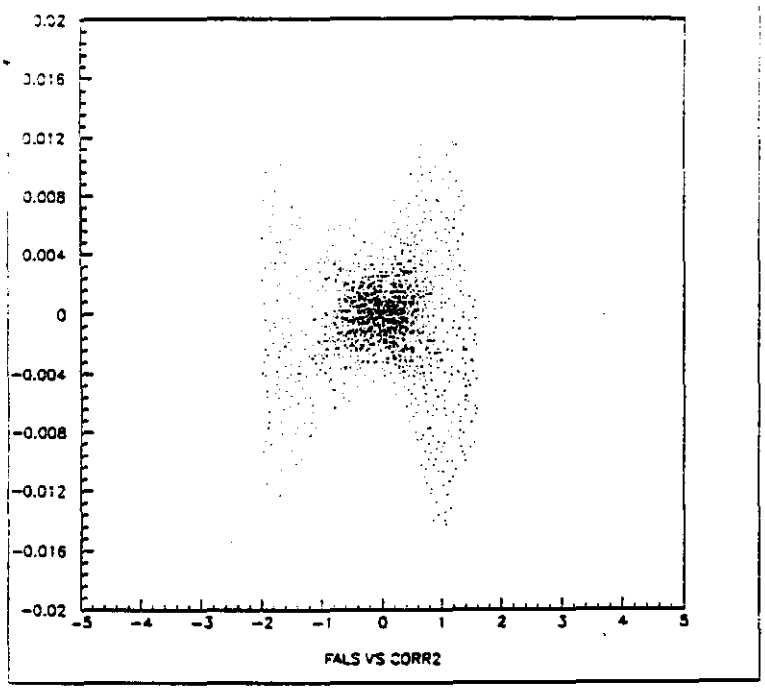

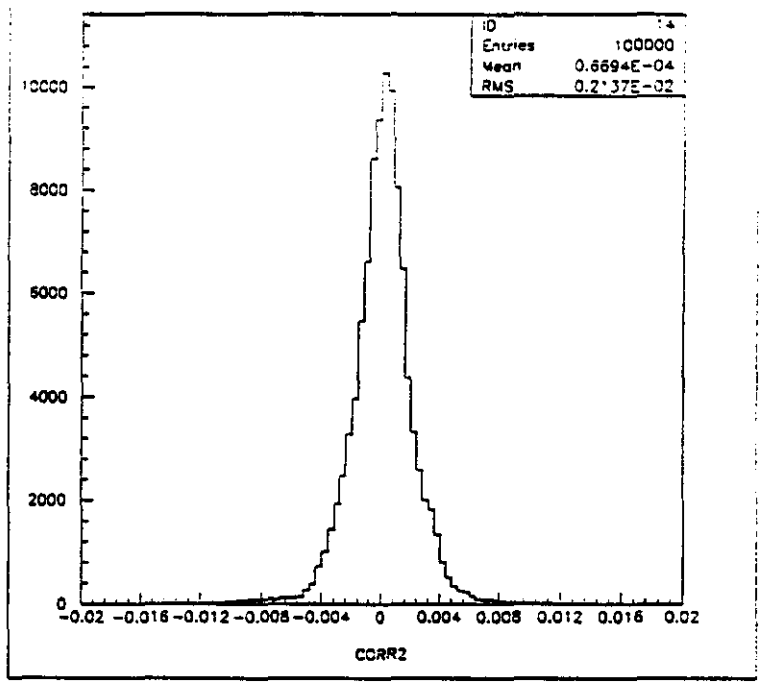

'ig.14a Corrected Sagitta(cm) vs False Sagitta(cm)

Fig.14b Corrected Sagitta(cm)

Shifts and Rotations of Muon Chambers: $Dx, Dy, Dz \leq \pm 5mm$; $Sx, Sy, Sz \leq \pm 3mrad$

Deformations of Muon Chambers: $\Psi_{torqe} \leq \pm 3mrad$, $\Delta t^0 \leq \pm 5^0$

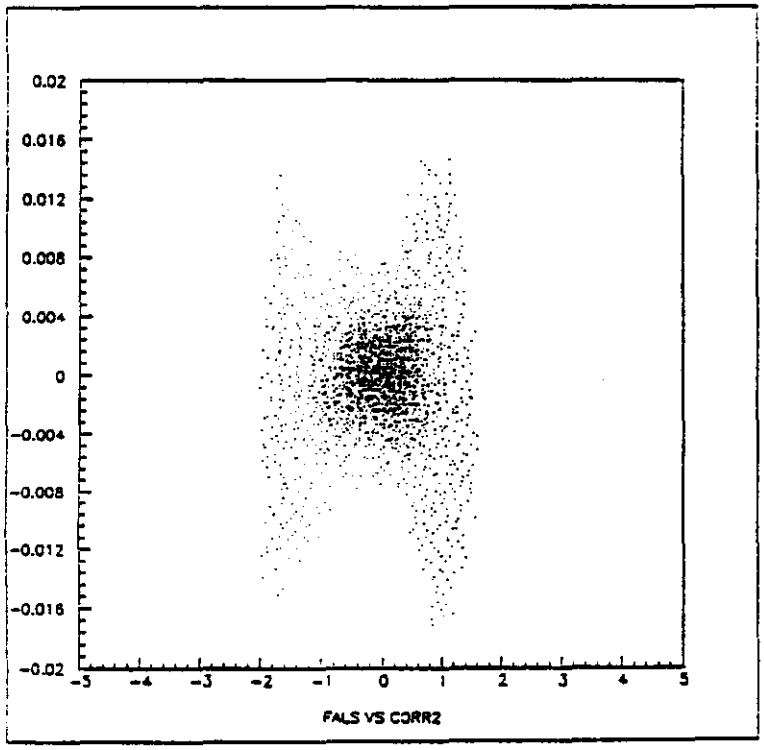

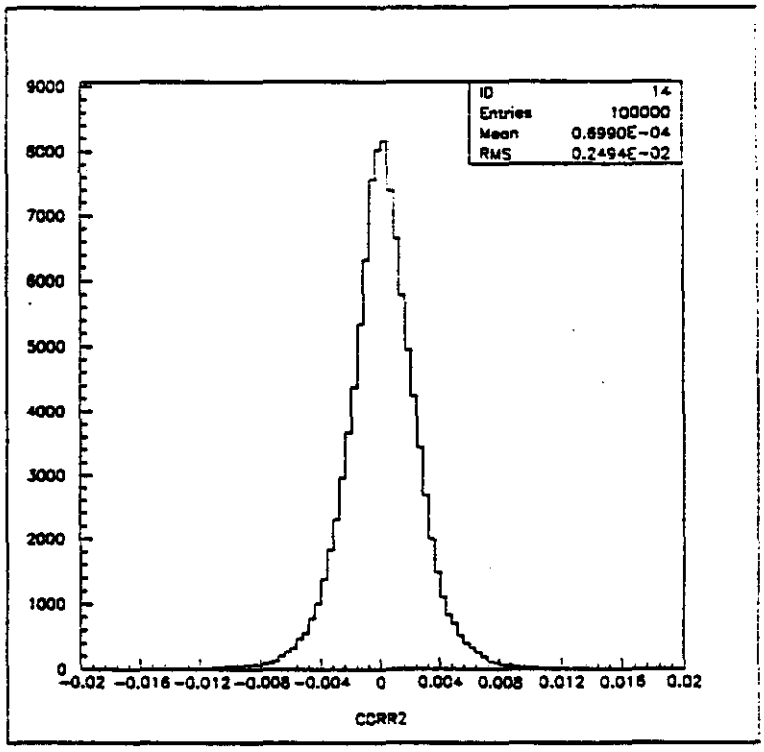

ig.15a Corrected Sagitta(cm) vs False Sagitta(cm)

Fig.15b Corrected Sagitta(cm)

Shifts, Rotations and Deformations of Muon Chambers as for Fig.14

Non-Projectivity of Particle Trajectory: $\Delta X_{IP} \leq \pm 1cm; \Delta Z_{IP} \leq \pm 5cm$

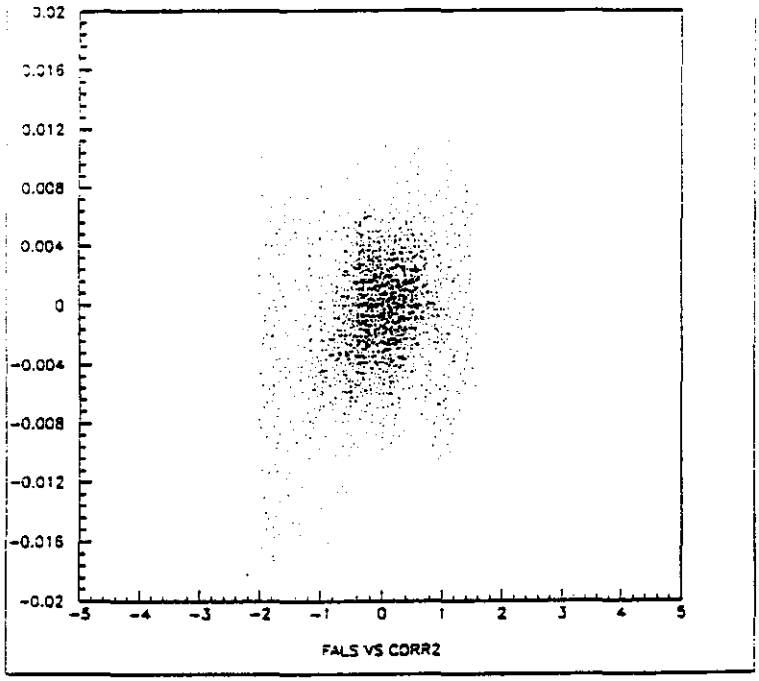

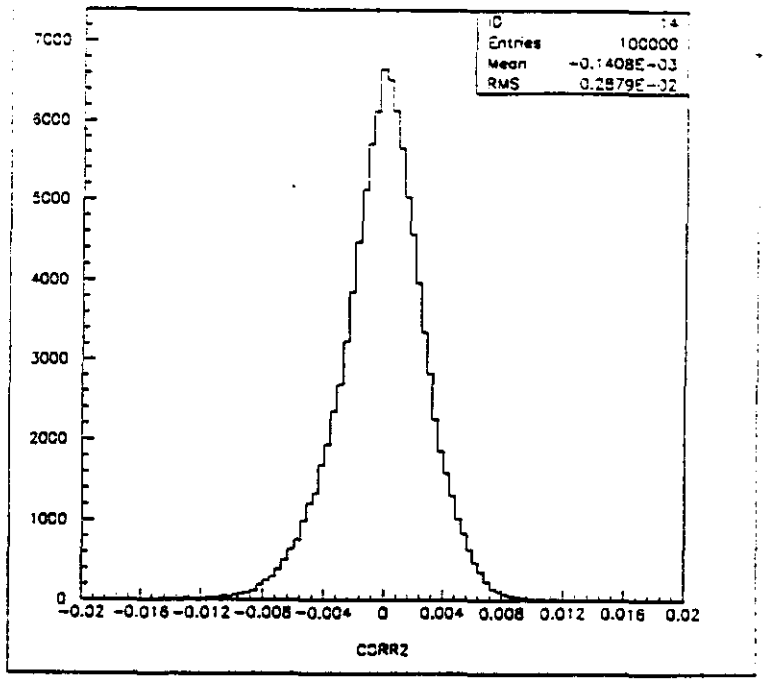

ig.16a Corrected Sagitta(cm) vs False Sagitta(cm)

Fig.16b Corrected Sagitta(cm)

Shifts, Rotations and Deformations of Muon Chambers as for Fig.14

Deflection of Muon Tower Focus from Interaction Point: $X_{focus} = 3cm; Y_{focus} = 3cm; Z_{focus} = 3cm$

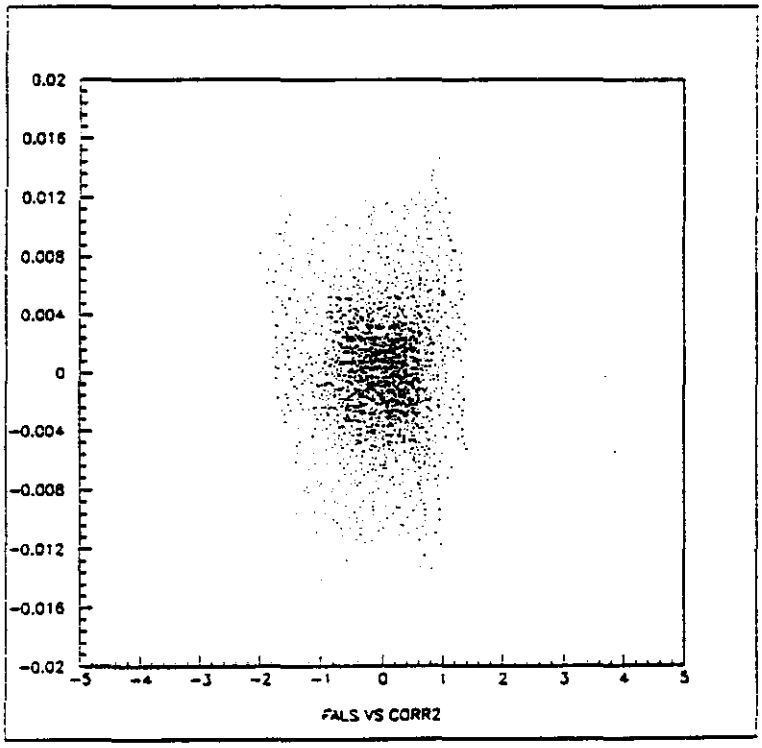

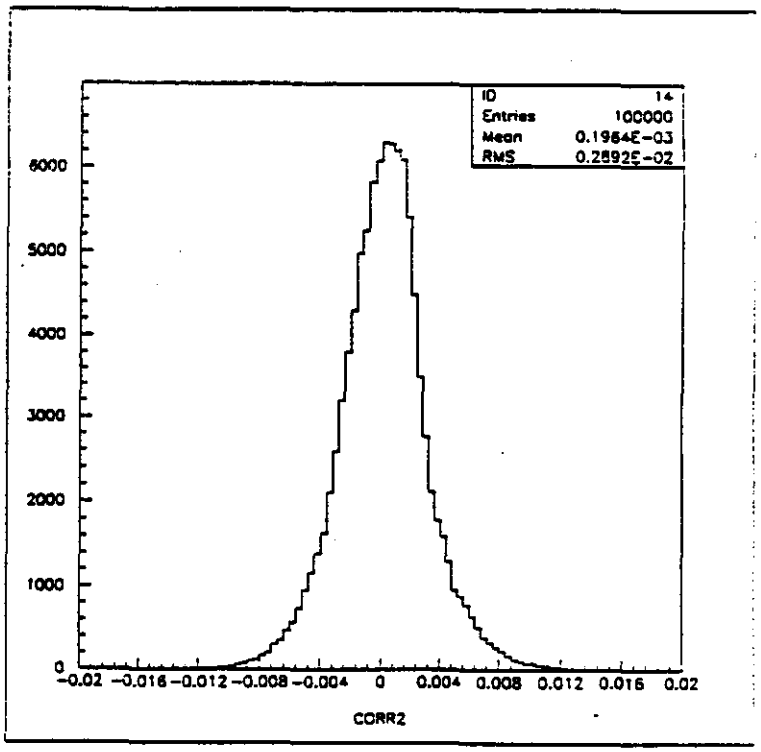

'ig.17a Corrected Sagitta(cm) vs False Sagitta(cm)

Fig.17b Corrected Sagitta(cm)

Shifts, Rotations and Deformations of Muon Chambers as for Fig.14

Deflection of Monitor Direction from Interaction Point: $\Delta\theta \leq \pm 3mrad$

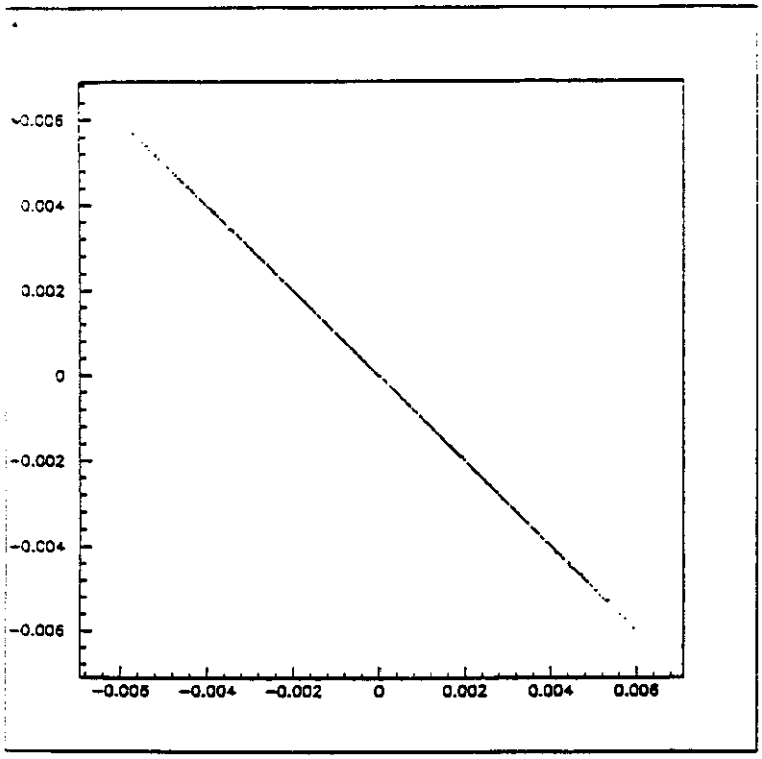

Fig.18 $b_{10} vs a_{01}$

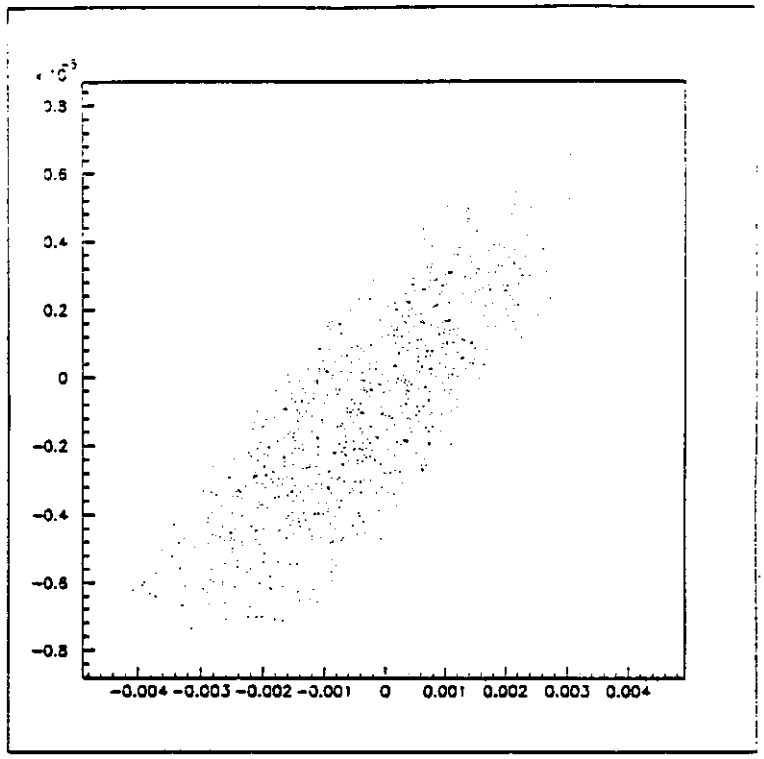

Fig.19 $b_{01} vs a_{11}$

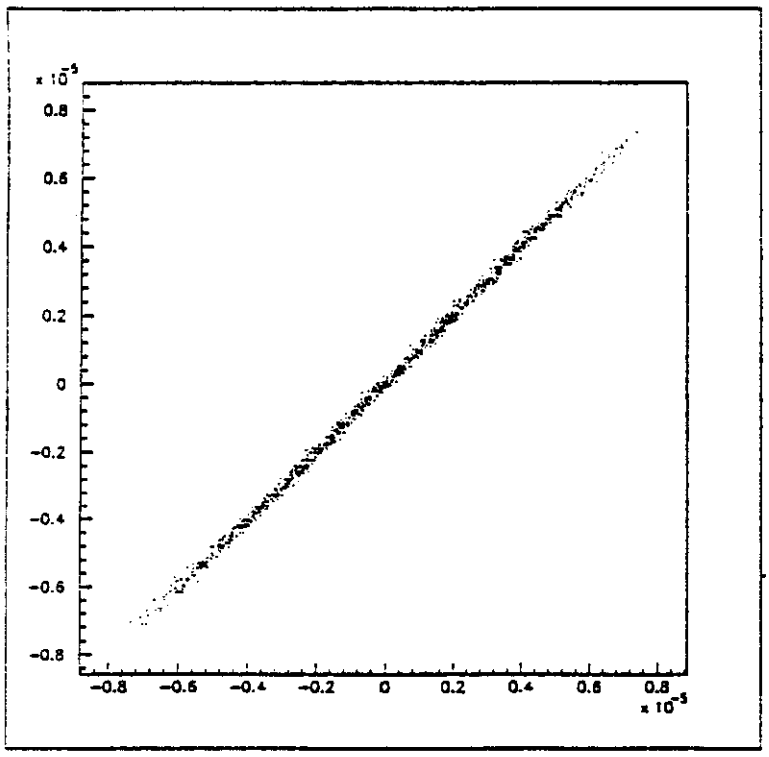

Fig.20 $b_{11} vs a_{02}$; **No Torsion**

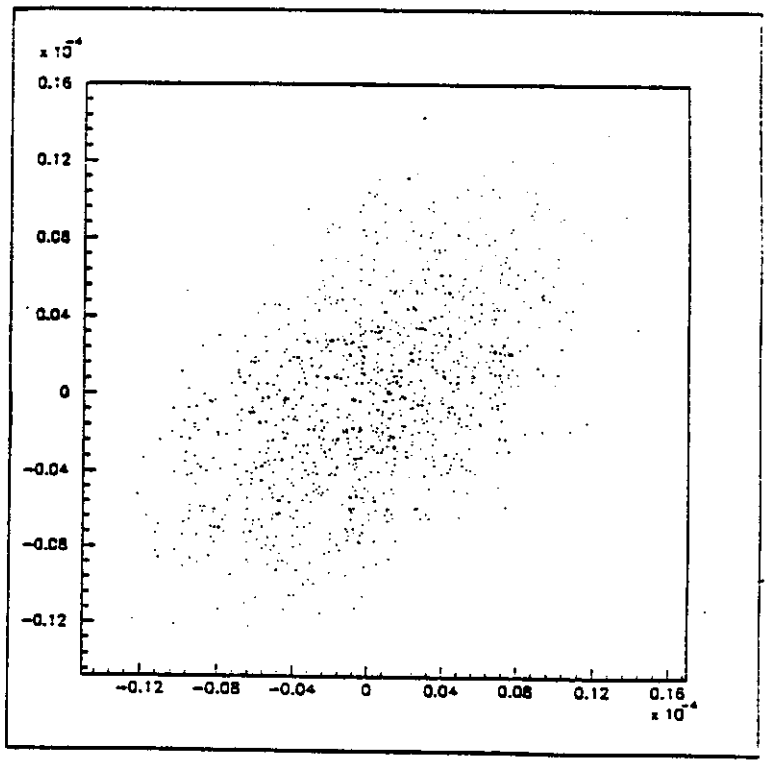

Fig.21 $b_{11} vs a_{02}$; **Torsion:** $\Psi_{torqe} \leq \pm 3 mrad$